Multi-quasiparticle sub-nanosecond isomers in ^{178}W

M. Rudigier, P.M. Walker, R.L. Canavan, Zs. Podolyák, P.H. Regan, P.-A. Söderström, M. Lebois, J.N. Wilson, N. Jovancevic, A. Blazhev, et al.

Physics Letters B 801 (2020) 135140

Contents lists available at ScienceDirect

Physics Letters B

www.elsevier.com/locate/physletb

Multi-quasiparticle sub-nanosecond isomers in ^{178}W

M. Rudigier [a,*], P.M. Walker [a,**], R.L. Canavan [a,b], Zs. Podolyák [a], P.H. Regan [a,b], P.-A. Söderström [c,d], M. Lebois [e,f], J.N. Wilson [e,f], N. Jovancevic [e,f], A. Blazhev [g], J. Benito [h], S. Bottoni [i], M. Brunet [a], N. Cieplicka-Orynczak [j], S. Courtin [k], D.T. Doherty [a], L.M. Fraile [h], K. Hadynska-Klek [a], M. Heine [k], Ł.W. Iskra [i,j], J. Jolie [g], V. Karayonchev [g], A. Kennington [a], P. Koseoglou [c,d], G. Lotay [a], G. Lorusso [a,b], M. Nakhostin [a], C.R. Nita [l], S. Oberstedt [m], L. Qi [e,f], J.-M. Régis [g], V. Sánchez-Tembleque [h], R. Shearman [a,b], W. Witt [c,d], V. Vedia [h], K.O. Zell [g]

[a] Department of Physics, University of Surrey, Guildford, GU2 7XH, UK
[b] National Physical Laboratory, Teddington, Middlesex, TW11 0LW, UK
[c] Institut für Kernphysik, Technische Universität Darmstadt, Schlossgartenstrasse 9, 64289, Darmstadt, Germany
[d] GSI Helmholtzzentrum für Schwerionenforschung GmbH, 64291 Darmstadt, Germany
[e] Institut de Physique Nucléaire, CNRS-IN2P3, Univ. Paris-Sud, Université Paris-Saclay, 91406 Orsay Cedex, France
[f] Université Paris-Saclay, 15 Rue G. Clémenceau, 91406 Orsay Cedex, France
[g] Institut für Kernphysik der Universität zu Köln, Zülpicher Strasse 77, D-50937 Köln, Germany
[h] Universidad Complutense, Grupo de Física Nuclear and UPARCOS, CEI Moncloa, E-28040 Madrid, Spain
[i] Dipartimento di Fisica, Università degli Studi di Milano and INFN sez. Milano, I-20133, Milano, Italy
[j] Institute of Nuclear Physics, Polish Academy of Sciences, PL-31-342 Kraków, Poland
[k] IPHC and CNRS, Universite de Strasbourg, F-67037 Strasbourg, France
[l] Horia Hulubei National Institute of Physics and Nuclear Engineering (IFIN-HH), R-077125 Bucharest, Romania
[m] European Commission, Joint Research Centre, Directorate G, Retieseweg 111, 2440 Geel, Belgium

ARTICLE INFO

Article history:
Received 4 July 2019
Received in revised form 30 September 2019
Accepted 2 December 2019
Available online 11 December 2019
Editor: D.F. Geesaman

ABSTRACT

We report on the first measurement of the half-lives of $K^\pi = 11^-$ and 12^+ four-quasiparticle states in the even-even nucleus ^{178}W. The sub-nanosecond half-lives were measured by applying the centroid shift method to data taken with $LaBr_3$(Ce) scintillator detectors of the NuBall array at the ALTO facility in Orsay, France. The half-lives of these states only became experimentally accessible by the combination of several experimental techniques - scintillator fast timing, isomer spectroscopy with a pulsed beam, and the event-by-event calorimetry information provided by the NuBall array. The measured half-lives are 476(44)ps and 275(65)ps for the $I^\pi = 11^-$ and 12^+ states, respectively. The decay transitions include weakly hindered $E1$ and $E2$ branches directly to the ground-state band, bypassing the two-quasiparticle states. This is the first such observation for an $E1$ transition. The interpretation of the small hindrance hinges on mixing between the ground-state band and the t-band.

1. Introduction

The $A \approx 180$ region of deformed nuclei exemplifies the competition between individual-particle and collective degrees of freedom [1]. A key aspect is that the projection of the angular momentum, K, on the nuclear symmetry axis is approximately conserved, and this gives rise to K isomers when the change in K-value, ΔK, exceeds the multipole order of the decay radiation, λ. Such transitions are called "K-forbidden", and the degree of forbiddenness is defined as $\nu = \Delta K - \lambda$. An extreme case is the $T_{1/2} = 31$ y, $K^\pi = 16^+$ isomer in ^{178}Hf at an excitation energy of 2446 keV [2], which is 989 keV *below* the $K = 0$, $I^\pi = 16^+$ collective rotation of the ground-state band (GSB). The 31-y isomer has a structure based on two broken nucleon pairs, i.e. it is a four-quasiparticle (4qp) state.

However, the competition between individual-particle and collective excitations changes quickly with nucleon number. In ^{178}W, for example, with two more protons and two fewer neutrons, the longest-lived 4qp state ($K^\pi = 15^+$) observed to date has a half-life

* Principal corresponding author.
** Corresponding author.
E-mail addresses: mat.rudigier@gmail.com (M. Rudigier), p.walker@surrey.ac.uk (P.M. Walker).

https://doi.org/10.1016/j.physletb.2019.135140

of just 30 ns, and there are other 4qp states (e.g. $K^\pi = 11^-$ and 12^+) with half-lives that have been too short to measure in previous studies ($T_{1/2} \leq 2$ ns and ≤ 1 ns, respectively) [3]. Furthermore, these two states lie at excitation energies considerably above the yrast line (the 12^+ state is 991 keV *above* the 12^+ GSB member) and they have highly K-forbidden decay branches directly to the GSB, bypassing the 2qp states. The bypassing transitions demonstrate an apparent collapse of the goodness of the K quantum number, thus providing extreme examples of so-called "anomalous" decays that were first identified from the 6qp, $T_{1/2} = 130$ ns isomer in ^{182}Os [4], and the 4qp, $T_{1/2} = 3.7$ µs isomer in ^{174}Hf [5].

It has been a long-standing experimental challenge to measure the short half-lives of the $K^\pi = 11^-$ and 12^+ states in ^{178}W, so that the extreme nature of their anomalous decays can be quantified. Hence, it would be possible to understand better the way in which the K quantum number is broken down. However, the level structure of ^{178}W and its γ-ray spectra are complex, and the non-yrast location of the 4qp states leads to weak population. Nevertheless, as we now report, by exploiting a pulsed beam and a reaction that populates higher-lying isomers, together with an array of $LaBr_3$(Ce) detectors combined with Ge detectors, and advanced analysis techniques, it has been possible to measure the half-lives of these states.

2. Experimental conditions

The experiment was performed at the ALTO accelerator facility at the IPN Orsay, France. A beam of ^{18}O ions was impinged on a 6.3 mg/cm^2 target of enriched ^{164}Dy with a 1 mg/cm^2 Au backing. The beam consisted of bunched 2 ns long pulses with 400 ns repetition period. The strongest channels were ^{164}Dy(^{18}O, 4n)^{178}W and Coulomb excitation of the target nucleus. During the six-day measurement about equal time was used for three different beam energies, 71 MeV, 76 MeV, and 80 MeV. The Coulomb barrier lies at 72 MeV. The data taken with the beam energy at 71 MeV were not included in the current analysis.

Decay γ radiation was detected with the NuBall array [6] which was set up for a long campaign at Orsay that lasted from November 2017 until late summer of 2018. The array consisted of 24 Clover detectors close to 90 degrees with respect to the beam axis. There were 10 co-axial HPGe detectors at backward angles, and 20 $LaBr_3$(Ce) detectors at forward angles.

Data acquisition was fully digital and implemented with the "FASTER" system [7]. The γ-γ time resolution (FWHM) of the Ge and $LaBr_3$ detectors, measured with a ^{60}Co source, was 20 ns and 320 ps respectively. This was the first experiment of the NuBall campaign. The detector and electronics setup was slightly different with respect to the later measurements with the LICORNE neutron source [8]. The differences shall briefly be highlighted here. There were two categories of $LaBr_3$(Ce) crystals, 10 of truncated cone shape, 1.5" in length and 1" and 1.5" at the bases [9] and 10 of the UK FATIMA type with cylindrical shape and dimensions 1.5"×2" [10], both using the same R9779 photo multiplier tube (PMT) from Hamamatsu. The conical detectors had a 1 mm layer of lead shielding around the crystal. No other shielding was present between the $LaBr_3$ detectors. Only the $LaBr_3$ detector channels in the data acquisition had a digital CFD for time walk minimisation and sub-nanosecond time pick-off. This means that walk correction for Ge and BGO detectors was performed offline. For the $LaBr_3$ detectors a residual time walk correction (on the picosecond scale) was applied offline (see below). In contrast to later experiments in the campaign a global trigger was used. The trigger condition was (one $LaBr_3$ AND one Ge) OR (two $LaBr_3$) detectors within a window of 2 µs.

In general conditions during the experiment were very stable. In particular we did not observe a significant gain drift in the $LaBr_3$ energy spectra during the measurements with each individual beam energy. However, we observed gain shifts between the different energy runs, which we attribute to different γ ray rates.

3. Data analysis and results

The aim of this analysis was to obtain the lifetimes of short-lived sub-nanosecond isomers in ^{178}W. From previous measurements using Ge detectors some of these levels were known to have lifetimes shorter than a couple of nanoseconds [3,11]. The better time resolution of $LaBr_3$(Ce) scintillator detectors makes a delayed γ-γ coincidence lifetime measurement using the centroid shift method [12] possible. This method is well established and based on the fact that the centroid C of a delayed time distribution is shifted with respect to that of a corresponding prompt time distribution C_{Prompt} by the mean lifetime τ of the intermediate state:

$$C^* = C - C_{\text{Prompt}} = \tau .$$

Measurements with ^{60}Co and ^{152}Eu sources were used for energy, efficiency, and timing calibration. The precise determination of the residual prompt response time walk for the $LaBr_3$ detectors is crucial for sub-nanosecond lifetime measurements with the centroid shift method [13]. By measuring previously reported lifetimes in ^{164}Dy it was demonstrated that the calibration taken with the ^{152}Eu source holds under in-beam conditions [14]. The same publication [14] contains a figure of the prompt response timewalk $C_{\text{Prompt}}(E_\gamma)$ which was used in this work.

Coincidences between neighbouring detectors, which are dominated by Compton scattering between crystals, were excluded from the analysis.

The study of the decay of long-lived isomers in ^{178}W is facilitated through the pulsed beam. This allows the selection of γ rays that are emitted after population of long-lived isomers, of which there are several at energies above 3 MeV in ^{178}W, e.g. the 15^+ state at 3654 keV with $T_{1/2}$ = 30 ns or the 21^- state at 5314 keV with $T_{1/2}$ = 64 ns [3].

By selecting γ rays that were emitted outside of the prompt time region around a beam pulse, the coincidence spectra can be cleaned up significantly. In this way it is possible to perform γ-γ delayed coincidence measurements out of beam. Doing this with the $LaBr_3$ detectors enables us to measure the lifetime of short lived isomers in these very complex excitation spectra for the first time. Statistics was not sufficient to allow an additional energy gate on the Ge detectors.

One significant feature of the NuBall array is the fact that the BGO crystals surrounding the Ge detectors were not shielded towards the target position. The intention of this was to use them as an additional source of information for calorimetry studies. In an analysis like the present one it can be used as a powerful channel selection tool, as it provides us with a high-efficiency multiplicity filter. By setting conditions on the number of detected γ-rays for both the prompt and delayed part of an event, we were able to improve the peak-to-background ratio of our transitions of interest by a factor of up to 3.5, while at the same time reducing the total number of counts in the coincidence spectra only by a factor of about 2. The delayed time window was set from 40 ns to 270 ns after the beam pulse.

In our case the condition of prompt multiplicity ≥ 1 and delayed multiplicity ≥ 3 was found to be a good compromise between statistics and peak-to-background ratio for the study of the short lived isomers around 3 MeV in ^{178}W.

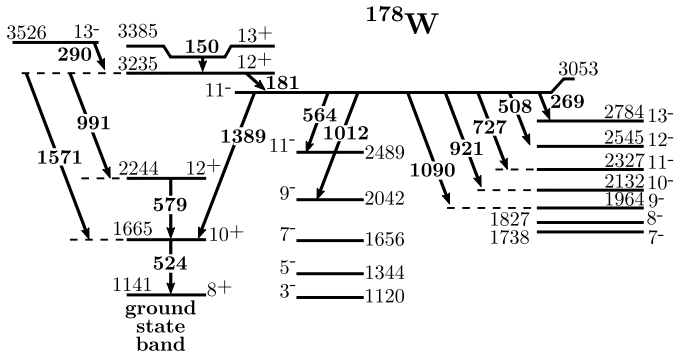

Fig. 1. Partial decay scheme of ^{178}W around the 12^+ and 11^- isomers studied in this work; some weak transitions were omitted. Data taken from [3].

With these conditions we identified two isomers whose lifetimes we were able to measure. Attempts to measure the lifetimes of other high-lying states, like the 18^- state at 4878 keV, or those of the states in the band of the 13^- level at 3523 keV were unfortunately not successful due to low statistics or contaminations.

We were able to set clean $LaBr_3$ energy gates on transitions populating and de-populating the 11^- isomer at 3053 keV, namely the γ cascades 181 keV - 921 keV and 181 keV - 1090 keV. See Fig. 1 for a partial level scheme of ^{178}W.

The lifetime of the 12^+ isomer at 3235 keV was not accessible in this direct way. Gating on the 290 keV transition, the peak of the coincident transition at 181 keV – connecting the state at 3235 keV with the state at 3053 keV – is contaminated significantly with a γ ray at energy 184 keV. These two transitions cannot be resolved in the $LaBr_3$ spectrum, which renders a direct coincidence measurement of this state's lifetime impossible in this case. Therefore, we took advantage of a general feature of the centroid shift method that has mainly been exploited in β-γ fast timing measurements before [12]. If the time difference spectrum of two transitions in a direct cascade going through states with lifetimes τ_1, τ_2, etc., is measured, then the centroid C^* of this coincidence is actually shifted by just the sum of the lifetimes of the intermediate states

$$C^* = C - C_{\text{Prompt}} = \tau_1 + \tau_2 + ... \quad (1)$$

The coincidence cascade 290 keV - 921 keV is clean, and the same is true for 290 keV - 1090 keV. As we have already determined the lifetime of the 11^- state directly we can infer the lifetime of the 12^+ state using these coincidences via the above mentioned relation.

As can be seen from Figs. 2 and 3 there is still significant coincidence background – stemming mostly from Compton scattered coincident γ rays – which has to be treated accordingly. The peak-to-background ratio is 0.63 for Fig. 2 b), and 0.76 for Fig. 3 b). In all lifetime measurements in this work we applied the procedure described in ref. [15], where the background contribution to the centroid of the total time spectrum is separated into three parts. These are then individually estimated by setting energy gates outside of the coincidence region and interpolating the value at the peak position. Polynomial functions were used for interpolation, and the uncertainty was in each case estimated from the standard deviation of the fit residual. The centroid position for the full energy peak coincidence is then obtained by subtracting the background centroids with the appropriate weights from the total distribution. One advantage of this approach is that no assumptions about the shape of the background time distributions have to be made.

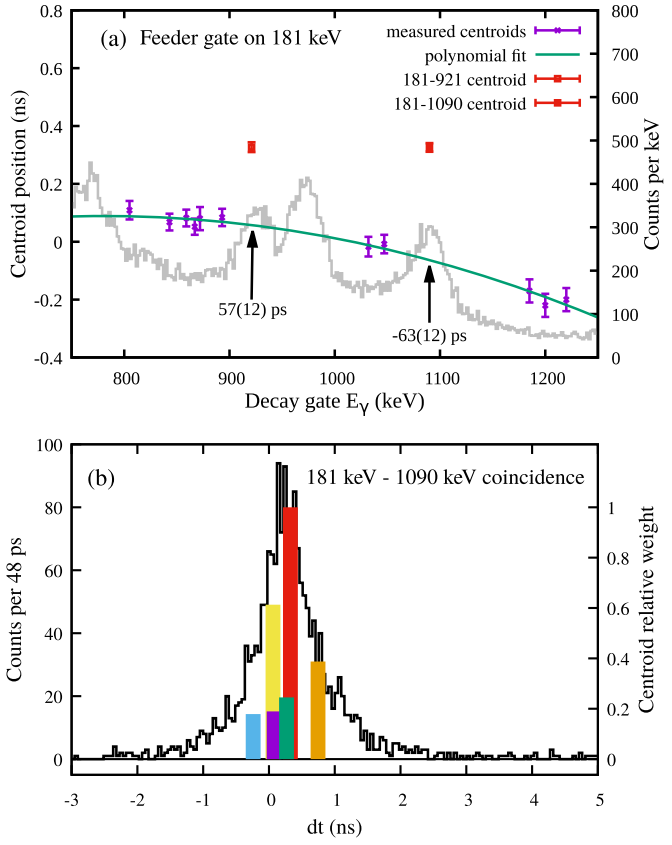

Fig. 2. (a) Centroid interpolation for the determination of one background component for the measurement of the lifetime of the $K^\pi = 11^-$ isomer at 3053 keV. The positions of the two coincident transitions of interest are marked with arrows. A gated $LaBr_3$ spectrum is shown in grey. (b) Raw time difference spectrum obtained with a $LaBr_3$ coincidence gate on the 181 keV and 1090 keV transitions (black). The centroid of the total distribution is shown as a red bar. The centroids of the three background components, determined via interpolation (see text) are shown in green, blue and purple. The total background centroid is shown in yellow. The deduced centroid for the background-corrected delayed coincidence is shown in orange.

With this background corrected centroid value the lifetime can then be determined by applying the prompt response correction, which was obtained from the ^{152}Eu calibration [14]. The results for the individual measurements are given in Table 1. The contribution of the prompt response correction to the uncertainty of the lifetime is of the order of 10 ps (7 ps for the half-life).

From the results in Table 1 we calculated a weighted mean for both lifetimes. The half-lives are 476(44) ps and 275(65) ps for the 11^- and 12^+ isomers (Table 2), respectively. While these are short compared to typical K isomers, they at least indicate that intrinsic (quasiparticle) states are involved, and it is reasonable to assign the K values as being equal to the spin values. Relative γ intensities were measured using the Ge detectors. Conversion coefficients were calculated using the BrIcc code [16]. The obtained reduced hindrance factors f_ν for the transitions depopulating the 3235 keV and 3053 keV levels are shown in Tables 3 and 4. Here, f_ν is defined as the νth root of the Weisskopf hindrance factor [1,2]. Note also that the assumption of pure multipoles is for the purpose of evaluating conversion coefficients and f_ν values. In the case of $M1$ transitions, significant $E2$ admixtures are possible, but these have not been measured. In fact, for the present data, the f_ν values for the other transitions, i.e. $E1$ and stretched $E2$, are not affected (within error bars) by this assumption.

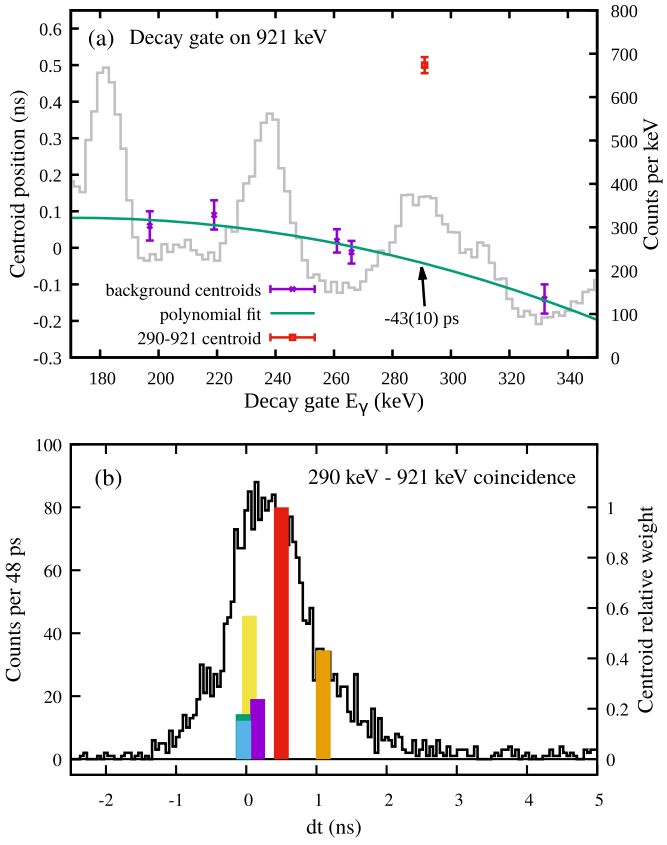

Fig. 3. (a) Centroid interpolation for the determination of one timing background component for the 290 keV - 921 keV cascade. The position of the coincident transition at 290 keV is marked with an arrow. The uncertainty was determined from the standard deviation of the fit residual. A gated $LaBr_3$ spectrum is shown in grey. (b) Raw time difference spectrum obtained with a coincidence gate on the 290 keV and 921 keV transitions (black). The centroid of the total distribution is shown as a red bar. The centroids of the three background components, determined via interpolation, are shown in green, blue and purple. The total background centroid is shown in yellow. The deduced centroid for the background-corrected delayed coincidence is shown in orange.

Table 1
Centroid values C^* for the indicated γ-γ coincidences. The measured values C are corrected for background contribution and the corresponding prompt centroid position.

$E_{\gamma,1}$ (keV)	$E_{\gamma,2}$ (keV)	C^* (ps)
290	921	1094(84)
290	1090	1067(121)
181	921	651(95)
181	1090	718(84)

Table 2
Final results of measured lifetimes. For 11^-: weighted average of two measurements. For 12^+: difference of weighted averages according to Eq. (1).

I^π	E_{Level} (keV)	τ (ps)	$T_{1/2}$ (ps)
12^+	3235	397(93)	275(65)
11^-	3053	687(63)	476(44)

4. Discussion

4.1. The low E2 hindrance from the 12^+ isomer to the GSB

The variation of reduced hindrance with proton number is shown in Fig. 4. The figure includes all $E1$ and $E2$ "bypassing" transitions from 4qp isomers in even-even nuclides, directly to the GSB, i.e. bypassing the 2qp states. The general trend of decreasing f_ν with increasing Z could be due to increasing gamma softness [1,2]. Nevertheless, it is evident that all the values are low ($f_\nu < 6$). Here the focus is on the ^{178}W value, which is even lower than might be expected from the trend of the data, but first we recall the situation for ^{174}Hf.

Table 3
Reduced hindrance factors f_ν measured in this work for transitions depopulating the 11^- state at 3053 keV in ^{178}W. Pure multipoles $\sigma\lambda$ are assumed. The γ branching ratio b is based on measured relative γ ray intensities and theoretical conversion coefficients for the stated multipole orders. Transition strengths of E1 character were corrected by a factor of 10^4 for comparability (see discussion for details).

Decay to						
I^π_{final}	E_{final} (keV)	E_γ (keV)	$\sigma\lambda$	ν	b (%)	f_ν
10^+	1665	1389	$E1$	10	1.9(4)	2.80(8)
9^-	1964	1090	$E2$	2	33(4)	15(1)
9^-	2041	1012	$E2$	7	2.0(4)	3.1(1)
10^-	2133	921	$M1$	3	29(3)	39(2)
11^-	2328	727	$M1$	3	3.6(7)	61(4)
11^-	2490	564	$M1$	8	2.9(6)	4.4(1)
12^-	2546	508	$M1$	3	8(1)	33(2)
10^-	2578	476	$M1$	2	11(1)	148(11)
13^-	2784	269	$E2$	2	1.0(6)	2.6(8)
11^-	2842	212	$M1$	2	4.1(5)	71(5)

Table 4
Same as Table 3 but for the 12^+ state at 3235 keV in ^{178}W. The K value of the 12^+ state at 2845 keV was assumed to be 8, based on the discussion in [3] (see text).

Decay to						
I^π_{final}	E_{final} (keV)	E_γ (keV)	σL	ν	b (%)	f_ν
10^+	1664	1571	$E2$	10	6.9(12)	2.30(7)
12^+	2244	991	$M1$	11	4.8(9)	3.09(9)
11^-	2327	908	$E1$	4	1.1(3)	9.6(10)
10^+	2444	791	$E2$	4	3.8(9)	3.9(3)
12^-	2546	689	$E1$	4	1.0(4)	8.0(11)
11^+	2671	564	$M1$	5	3.7(9)	9.0(6)
10^+	2683	552	$E2$	2	8.1(15)	4.3(7)
12^+	2804	431	$M1$	11	3.1(8)	2.57(8)
12^+	2845	390	$M1$	(3)	2.4(6)	31(4)
11^-	3053	181	$E1$	0	59(10)	-

The ^{174}Hf value was discussed [5] in terms of mixing with an isolated $(i_{13/2})^2$ s-band state at $I = 12$, though now it would be more appropriate to give a t-band interpretation (where the Fermi-aligned $i_{13/2}$ neutrons have significant K projections – see [17] for a recent summary of t-band structures). Either way, when the high-K structure of the $(i_{13/2})^2$ admixture is not explicitly taken into account, there is the appearance of low reduced hindrance for the $E2$ decay to the GSB.

In a similar way, there is t-band mixing in ^{178}W [3]. Importantly, in this case the yrare (energetically unfavoured) band for $I \geq 12$ has been identified as a t-band with $K \approx 8$. The high-K value was extracted by Purry et al. [3] from an analysis of the $E2$ branching ratios in the crossing region with the GSB, and a GSB/t-band mixing matrix element of 68 keV was obtained. Although the $I = 10$ member of the t-band was not assigned, this could plausibly be the $I^\pi = 10^+$ state at 2682 keV, which is fed from the $K^\pi = 12^+$ isomer by a 552 keV, $E2$ transition. If the 2682 keV state has $K = 8$ from the $(i_{13/2})^2$, $\{\frac{7}{2}^+[633], \frac{9}{2}^+[624]\}$ t-band coupling, then the 552 keV transition has $\nu = 2$, and $f_\nu = 4.3$. This is already a low value, but we note that the configuration of the 12^+ isomer itself involves two $i_{13/2}$ neutrons $\{\frac{7}{2}^+[633], \frac{9}{2}^+[624]\}$ coupled

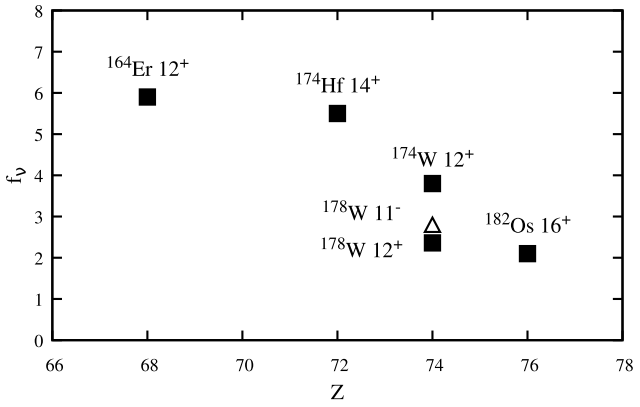

Fig. 4. Reduced hindrance values for $E2$ (filled symbols) and $E1$ (open symbol) transitions which go directly from 4qp isomers, with the given K^π values, to their respective GSB, bypassing the 2qp states. For the $E1$ transition, the Weisskopf hindrance has been divided by 10^4 (see text). Error-bars are smaller than symbols. The data are from [2–5,19,20] and the present work. Note that the reduced hindrance dependence on the energy relative to a rigid rotor [1,21], and a γ-tunneling model interpretation [20,22], provide alternative perspectives.

to $K = 8$ [3,18], which is just the t-configuration, so that the decay to the 2682 keV level would require only a simple recoupling of the two other neutrons in the 4qp configuration.

Using the 68 keV mixing matrix element obtained by Purry et al. [3], the 10^+ GSB member at 1665 keV can be calculated in a two-level-mixing scenario to have a 0.5% t-band, $< K > \approx 8$ admixture. If that 0.5% component accounts for the observed 1571 keV transition from the 12^+ isomer to the GSB, but the reduced hindrance is calculated with $K = 0$ for the GSB (as would usually be done) then an apparent reduced hindrance of f_ν = 2.3 is predicted, which is exactly the observed value. While there are uncertainties in the assumptions used, the general understanding appears to be good: there is a small t-band admixture in the GSB, which enables the direct transition to proceed from the 12^+ isomer, and this transition may be facilitated by the particular structure of the 4qp isomer, which includes the 2qp, t-band configuration. Note that in the ^{174}Hf case, there is no experimental evidence for the K value of the $I = 12$ mixing state. Therefore the present case of ^{178}W, with $K \approx 8$ for the t-band consistent with $E2$ branching ratios [3], has special significance for understanding the nature of bypassing transitions.

It would be desirable to apply the same procedure with the other 4qp isomers that have bypassing decays, i.e. those illustrated in Fig. 4. However, for ^{164}Er [19], ^{174}W [20] and ^{182}Os [4], there are no observed $E2$ decay branches to the corresponding yrare states, so that a different kind of analysis would be required, involving different assumptions. From an experimental perspective, it would be valuable to identify these missing transitions.

Note also that the 991 keV, $\Delta I = 0$ transition to the 12^+ member of the ^{178}W GSB also has a very low reduced hindrance, f_ν = 3.1, assuming $M1$ character. This is slightly larger than for the competing $E2$ transition to the 10^+ GSB member, with f_ν = 2.3. Such a difference between competing $M1$ and $E2$ K-forbidden decays is typical [2], but a quantitative discussion of the difference is inhibited by the lack of knowledge of the $E2/M1$ mixing ratio of the $\Delta I = 0$ transition.

4.2. The low $E1$ hindrance from the 11^- isomer to the GSB

The $E1$ reduced hindrance, from the 11^- isomer directly to the 10^+ member of the GSB, $f_\nu = 2.8$, is very small – indeed, it is the smallest value yet observed for any K-forbidden $E1$ transition, and it is the only example of a bypassing $E1$ transition to the GSB in an even-even nuclide. With the commonly employed 10^4 reduction applied to the $E1$ Weisskopf hindrance factor [23,24], similar $E2$ and (effective) $E1$ reduced hindrances are typically found, and this is certainly supported by the presently obtained values of f_ν = 2.3 and 2.8, respectively.

The 11^- isomer configuration involves the $\frac{9}{2}^+[624]$, $i_{13/2}$ neutron [3,18], but not both the $i_{13/2}$ neutrons of the t-configuration, as is evident for the 12^+ isomer. Nevertheless, the same t-band mixing at $I = 10$ introduces high-K components into the GSB 10^+ state, which can account for the small apparent f_ν value for the $E1$ transition (though a quantitative evaluation of the reduced hindrance would require additional assumptions).

Finally, it is appropriate to consider whether there could be chance near-degeneracies involved, with states having the same spin and parity, but different K values. Suffice to say that, at least for the 12^+ and 11^- isomers, and the 10^+ GSB state, no such accidental degeneracies are known within an energy interval of 100 keV. However, with the two isomers being well above the yrast line, it remains a possibility that mixing with as-yet unobserved states could play a role.

5. Conclusion

With γ-ray fast-timing techniques, short half-lives have been obtained for $K^\pi = 11^-$ (0.48 ns) and 12^+ (0.28 ns) 4qp states in ^{178}W, at excitation energies close to 3 MeV. Their highly K-forbidden decays directly to the 10^+ member of the GSB, bypassing the 2qp states, have very small reduced hindrance factors. These are interpreted as being at least partly due to mixing between the 10^+ GSB member and the 10^+ t-band state, which has a high-K structure based on two $i_{13/2}$ Fermi-aligned neutrons. The $E2$ result ($f_\nu = 2.3$) can be understood in a similar way to the long-standing value in ^{174}Hf, while the remarkably similar $E1$ result ($f_\nu = 2.8$) is a unique observation of its kind. Further experimental information is needed to enable a quantitative comparison of the K-mixing mechanism for bypassing decays in ^{164}Er, ^{174}W and ^{182}Os. In the meantime, the present work provides some of the best evidence to date that high-K admixtures in the GSB are key to understanding the apparent breakdown of the K quantum number.

Acknowledgements

Funding support is acknowledged from the UK Science and Technology Facilities Council under grant numbers ST/L005743/1 and ST/P005314/1, as well as the BMBF under grants NuSTAR.DA 05P15RDFN1, and 05P19PKFNA. This work was also supported by the Spanish gouvernment projects FPA2015-65035-P and RTI2018-098868-B-I00, as well as the project B2017/BMD-3888 PRONTO-CM. P.H. Regan acknowledges support from the UK Department of Business, Energy and Industrial Strategy (BEIS) via the Natioanl Measurement System (NMS). R.L. Canavan acknowledges support from the BEIS, and ENSAR2 transnational access funding from the European Commission.

References

[1] G.D. Dracoulis, P.M. Walker, F.G. Kondev, Rep. Prog. Phys. 79 (2016) 013010.
[2] F.G. Kondev, G.D. Dracoulis, T. Kibédi, At. Data Nucl. Data Tables 103–104 (2015) 50 105–106 (2015) 105 (erratum).
[3] C.S. Purry, P.M. Walker, G.D. Dracoulis, T. Kibédi, F.G. Kondev, S. Bayer, A.M. Bruce, A.E. Byrne, W. Gelletly, P.H. Regan, C. Thwaites, O. Burglin, N. Rowley, Nucl. Phys. A 632 (1998) 229.
[4] P. Chowdhury, B. Fabricius, C. Christensen, F. Azgui, S. Bjornholm, J. Borggreen, A. Holm, J. Pedersen, G. Sletten, M.A. Bentley, D. Howe, A.R. Mokhtar, J.D. Morrison, J.F. Sharpey-Schafer, P.M. Walker, R.M. Lieder, Nucl. Phys. A 485 (1988) 136.

[5] P.M. Walker, G. Sletten, N.L. Gjorup, M.A. Bentley, J. Borggreen, B. Fabricius, A. Holm, D. Howe, J. Pedersen, J.W. Roberts, J.F. Sharpey-Schafer, Phys. Rev. Lett. 65 (1990) 416.
[6] M. Lebois, N. Jovancevic, J.N. Wilson, D. Thisse, R. Canavan, M. Rudigier, Acta Phys. Pol. B 50 (2019) 425.
[7] D. Etasse, et al., Fast Acquisition SysTem for nuclEar Research, http://faster.in2p3.fr/index.php.
[8] N. Jovancevic, M. Lebois, J.N. Wilson, D. Thisse, L. Qi, I. Matea, F. Ibrahim, D. Verney, M. Babo, C. Delafosse, F. Adsley, G. Tocabens, A. Gottardo, Y. Popovitch, J. Nemer, R. Canavan, M. Rudigier, K. Belvedere, A. Boso, P. Regan, Z. Podolyák, R. Shearman, M. Bunce, P. Inavov, S. Oberstedt, A. Lopez-Martens, K. Hauschild, J. Ljungvall, R. Chakma, R. Lozeva, P.-A. Söderström, A. Oberstedt, D. Etasse, D. Ralet, A. Blazhev, R.-B. Gerst, G. Hafner, N. Cieplicka-Orynczak, L.W. Iskra, B. Fornal, G. Benzoni, S. Leoni, S. Bottoni, C. Henrich, P. Koseoglou, J. Wiederhold, I. Homm, C. Surder, T. Kroll, D. Knezevic, A. Dragic, L. Cortes, N. Warr, K. Miernik, E. Adamska, M. Piersa, K. Rezynkina, L. Fraile, J.B. Garcia, V. Sanchez, A. Algora, P. Davies, V. Guadilla-Gomez, M. Fallot, T. Kurtukian-Nieto, C. Schmitt, M. Heine, D.R. Tello, M. Yavachova, M. Diakaki, F. Zeiser, W. Paulson, D. Gestvang, Acta Phys. Pol. B 50 (2019) 297.
[9] V. Vedia, M. Carmona-Gallardo, L.M. Fraile, H. Mach, J.M. Udias, NIM A 857 (2017) 98.
[10] S. Lalkovski, A. Bruce, I. Burrows, D. Cullen, A. Grant, I. Lazarus, Z. Podolyák, V. Pucknell, P. Regan, M. Rudigier, J. Simpson, J. Smith 42 (2015) 593.
[11] D.M. Cullen, S.L. King, A.T. Reed, J.A. Sampson, P.M. Walker, C. Wheldon, F. Xu, G.D. Dracoulis, I.-Y. Lee, A.O. Macchiavelli, R.W. MacLeod, A.N. Wilson, C. Barton, Phys. Rev. C 60 (1999) 064301.
[12] H. Mach, R.L. Gill, M. Moszynski, Nucl. Instrum. Methods A 280 (1989) 49.
[13] J.-M. Régis, M. Dannhoff, J. Jolie, Nucl. Instrum. Methods A 897 (2018) 38.
[14] M. Rudigier, R.L. Canavan, P.H. Regan, P.-A. Söderström, M. Lebois, J.N. Wilson, N. Jovancevic, S. Bottoni, M. Brunet, N. Cieplicka-Orynczak, S. Courtin, D.T. Doherty, K. Hadynska-Klek, M. Heine, L.W. Iskra, V. Karayonchev, A. Kennington, P. Koseoglou, G. Lotay, G. Lorusso, M. Nakhostin, C.R. Nita, S. Oberstedt, Z. Podolyák, L. Qi, J.-M. Régis, R. Shearman, P.M. Walker, W. Witt, Acta Phys. Pol. B 50 (3) (2019) 661.
[15] E.R. Gamba, A.M. Bruce, M. Rudigier, Nucl. Instrum. Methods A 928 (2019) 93.
[16] T. Kibédi, T.W. Burrows, M.B. Trzhaskovskaya, P.M. Davidson, C.W. Nestor, Nucl. Instrum. Methods A 589 (2008) 202.
[17] P.M. Walker, F.R. Xu, Phys. Scr. 91 (2016) 013010.
[18] F.R. Xu, P.M. Walker, J.A. Sheikh, R. Wyss, Phys. Lett. B 435 (1998) 257.
[19] T.P.D. Swan, P.M. Walker, Z. Podolyák, M.W. Reed, G.D. Dracoulis, G.J. Lane, T. Kibédi, M.L. Smith, Phys. Rev. C 86 (2012) 044307.
[20] S.K. Tandel, P. Chowdhury, E.H. Seabury, I. Ahmad, M.P. Carpenter, S.M. Fischer, R.V.F. Janssens, T.L. Khoo, T. Lauritsen, C.J. Lister, D. Seweryniak, Y. Shimizu, Phys. Rev. C 73 (2006) 044306.
[21] P.M. Walker, D.M. Cullen, C.S. Purry, D.E. Appelbe, A.P. Byrne, G.D. Dracoulis, T. Kibédi, F.G. Kondev, I.Y. Lee, A.O. Macchiavelli, A.T. Reed, P.H. Regan, F. Xu, Phys. Lett. B 408 (1997) 42.
[22] K. Narimatsu, Y. Shimizu, T. Shizuma, Nucl. Phys. A 601 (1996) 69.
[23] Z. Patel, Z. Podolyák, P.M. Walker, P.H. Regan, P.-A. Söderström, H. Watanabe, E. Ideguchi, G.S. Simpson, S. Nishimura, F. Browne, P. Doornenbal, G. Lorusso, S. Rice, L. Sinclair, T. Sumikama, J. Wu, Z.Y. Xu, N. Aoi, H. Baba, F.L.B. Garrote, G. Benzoni, R. Daido, Z. Dombrádi, Y. Fang, N. Fukuda, G. Gey, S. Go, A. Gottardo, N. Inabe, T. Isobe, D. Kameda, K. Kobayashi, M. Kobayashi, T. Komatsubara, I. Kojouharov, T. Kubo, N. Kurz, I. Kuti, Z. Li, H.L. Liu, M. Matsushita, S. Michimasa, C.-B. Moon, H. Nishibata, I. Nishizuka, A. Odahara, E. Sahin, H. Sakurai, H. Schaffner, H. Suzuki, H. Takeda, M. Tanaka, J. Taprogge, Z. Vajta, F.R. Xu, A. Yagi, R. Yokoyama, Phys. Lett. B 753 (2016) 182.
[24] P.M. Walker, Phys. Scr. 92 (2017) 054001.